Topological organization of whole-brain white matter in HIV infection

Article *in* Brain Connectivity · January 2017

DOI: 10.1089/brain.2016.0457

Brain Connectivity

DOI: 10.1089/brain.2016.0457

Topological organization of whole-brain white matter in HIV infection

*Laurie M Baker[1], *Sarah A Cooley[2] (co-first author), Ryan P Cabeen[3], David H Laidlaw[4], John A Joska[5], Jacqueline Hoare[5], Dan J Stein[5,6], Jodi M Heaps-Woodruff[7], Lauren E Salminen[3], Robert H Paul[1,7]

[1]University of Missouri – Saint Louis, Department of Psychology, One University Boulevard, Stadler Hall 327, Saint Louis, MO 63121, 314-566-3761, lauriebaker@umsl.edu

[2]Washington University in Saint Louis, School of Medicine, Department of Neurology, Saint Louis, MO 63110

[3]University of Southern California, Keck School of Medicine, Los Angeles, CA 90032

[4]Brown University, Computer Science Department, Providence, RI 02912

[5]University of Cape Town, Department of Psychiatry and Mental Health, Cape Town, South Africa

[6] MRC Unit on Anxiety & Stress Disorders, Cape Town, South Africa

[7]Missouri Institute of Mental Health, St. Louis, MO 63134

*= contributed equally

Abstract

Infection with human immunodeficiency virus (HIV) is associated with neuroimaging alterations. However, little is known about the topological organization of whole-brain networks and the corresponding association with cognition. As such, we examined structural whole-brain white matter connectivity patterns and cognitive performance in 29 HIV+ young adults (mean age = 25.9) with limited or no HIV treatment history. HIV+ participants and demographically similar HIV– controls (n = 16) residing in South Africa underwent magnetic resonance imaging (MRI) and neuropsychological testing. Structural network models were constructed using diffusion MRI-based multi-fiber tractography and T_1-weighted MRI-based regional gray matter segmentation. Global network measures included whole-brain structural integration, connection strength, and structural segregation. Cognition was measured using a neuropsychological global deficit score (GDS) as well as individual cognitive domains. Results revealed that HIV+ participants exhibited significant disruptions to whole-brain networks, characterized by weaker structural integration (characteristic path length and efficiency), connection strength, and structural segregation (clustering coefficient) compared to HIV– controls (*p values* < 0.05). GDS scores and performance on learning/recall tasks were negatively correlated with the clustering coefficient ($p < 0.05$) in HIV+ participants. Results from the present study indicate disruption to brain network integrity in treatment limited HIV+ young adults with corresponding abnormalities in cognitive performance.

Keywords: HIV; cognition; whole-brain connectivity; network analysis

1.0 Introduction

The human immunodeficiency virus (HIV) crosses the blood brain barrier shortly after seroconversion (~8 days) and prior to marked immune suppression and overt cognitive dysfunction (Valcour et al., 2012). Despite the efficacy of combination antiretroviral therapy (cART) in reducing viral load, current treatments do not appear to prevent or reverse existing brain damage (Ances, Ortega, Vaida, Heaps, & Paul 2013; Harezlak et al., 2011; Heaton et al., 2011). Importantly, research shows axonal disruption and synaptic injury following HIV infection (Avdoshina, Bachis, & Mocchetti, 2013; Ellis, Langford, & Masliah, 2007; Everall et al., 1999; Everall et al., 2010; Masliah et al., 1997). Although specific brain regions appear uniquely vulnerable, HIV-mediated neuronal damage is present throughout the brain (Ellis, Langford, & Masliah, 2007; Ragin et al., 2004) and corresponds to neuropsychological dysfunction (Masliah et al., 1997).

Diffusion tensor imaging (DTI) provides a robust method for identifying disruptions to the structural connections throughout the brain. Multiple studies utilizing DTI reveal abnormalities in brain white matter capable of disrupting connectivity across brain regions in HIV+ individuals (Filippi et al., 2001, Ragin et al., 2004; Thurnher et al., 2005; Gongvatana et al., 2009; Hoare et al., 2011). Further, using complex network analysis, structural changes in white matter connections can be effectively modeled by combining diffusion magnetic resonance imaging (MRI)-based tractography and T_1-weighted MRI–based regional gray matter segmentation. This network-based approach is highly sensitive to alterations in brain integrity across multiple disease pathologies including schizophrenia, Alzheimer's disease, and major depressive disorder (Bullmore and Sporns 2009; Bassett et al., 2010; He et al., 2008; Lo et al., 2010; Zhang et al., 2011; Bassett et al., 2008; Yu et al., 2011).

Complex network analysis has been recently applied to investigate signatures of HIV neuropathogenesis (Jahanshad et al., 2012). In this study, significant disruptions to brain connectivity were identified in older HIV+ adults on cART. However, the relationship between the topological organization of white matter and cognitive function in HIV remains unclear. Further, no studies have examined connectivity metrics (e.g., structural segregation, structural integration, and connection strength) in younger HIV+ individuals. It is necessary to fill this gap in the literature in order to determine the functional relevance of white matter connectivity in HIV+ individuals, independent of advanced age.

We used diffusion MRI-based tractography and graph-theoretic approaches to investigate the topological organization of white matter in 29 HIV+ young adults and 16 HIV– demographically similar controls utilizing fiber-bundle length (FBL)-defined whole brain connectivity metrics (structural segregation, structural integration, and connection strength). These metrics provide insight into communication between regions of the brain. We also examined the relationship between whole-brain topological organization and cognitive performance using a global deficit score (GDS) and individual cognitive domain deficit scores (learning/recall, psychomotor/processing speed, executive function, fine motor skills and dexterity, and visuospatial skills). We hypothesized that whole-brain topological organization would be diminished in HIV+ individuals compared to HIV-controls, and the degree of abnormalities in the three connectivity metrics would significantly correlate with poorer cognitive performance in young HIV+ individuals.

2.0 Methods

2.1 Participants

HIV+ participants were recruited from primary care HIV clinics in Cape Town, South

Africa. Patients who were in the pretreatment counseling phase were identified from clinic records. Interested participants completed a comprehensive consent process followed by a detailed medical and demographic history. All participants were either treatment naïve at enrollment (83%), or had initiated cART within three months of enrollment (17%). All but five participants began treatment within one month of enrollment. HIV– participants were recruited from regional Voluntary Counseling and Testing Clinics in Cape Town, South Africa. Table 1 provides demographic information for the 29 HIV+ and 16 HIV– participants.

Inclusion criteria for HIV+ participants included: (1) age between the years of 18 and 45; (2) Xhosa as the primary language; (3) HIV serostatus documented by ELISA and confirmed by Western blot, plasma HIV RNA, or a second antibody test for the HIV+ group; and (4) at least 7 years of formal education (all but one participant reported at least 10 years of education). Exclusion criteria for all participants included (1) any major psychiatric condition that could significantly affect cognitive status (e.g., schizophrenia or bipolar disorder); (2) confounding neurological disorders including multiple sclerosis and other central nervous system (CNS) conditions; (3) head injury with loss of consciousness greater than 30 min; (4) clinical evidence of opportunistic CNS infections (toxoplasmosis, progressive multifocal leukoencephalopathy, neoplasms); and (5) current substance use disorder determined by the Mini-International Neuropsychiatric Interview Plus (MINIPlus) (Sheehan et al., 1998). All participants provided signed informed consent. Study procedures were approved by local university IRB committees.

2.2 HIV viral load and CD4 T-cell counts

EDTA blood samples were collected at the time of study visit and plasma and cell aliquots were stored at −70 °C. RNA was isolated from patient samples using the Abbott RealTime HIV-1 amplification reagent kit, according to the manufacturer's instructions. Viral

Topological organization of whole-brain white matter in HIV infection (doi: 10.1089/brain.2016.0457)
This paper has been peer-reviewed and accepted for publication, but has yet to undergo copyediting and proof correction. The final published version may differ from this proof.

load was determined using the Abbott m2000sp and the Abbott m2000rt analyzers (Abbott laboratories, Abbott Park, IL, USA). All HIV+ participants had a detectable viral load (range 183-1,759,510 copies/ml). Analyses of cells from fresh blood samples were completed on the FACSCalibur flow cytometer in conjunction with the MultiSET V1.1.2 software (BD Biosciences, San Jose, CA, USA) for CD4 T-cell counts.

2.3 Neuroimaging Acquisition

Neuroimaging was acquired on a 3T Siemens Allegra scanner (Siemens AG, Erlangen Germany), with a 4-channel phased-array head coil. Thirty unique diffusion gradient directions at b=1000 s/mm^2 were repeated to give a total of 60 diffusion weighted volumes using a customized single-shot multi-slice echo-planar tensor-encoded imaging sequence. Six baseline images were acquired and interleaved in the diffusion-weighted scans to improve motion-correction. Seventy contiguous slices were obtained per contrast with a 128 x 128 matrix and field of view of 218 x 218 mm (isotropic 1.7 x 1.7 x 1.7 mm^3 voxels); TR: 10s, TE: 103 ms using a full-Fourier transform. We also acquired a T_1-weighted 3-dimensional magnetization-prepared rapid acquisition gradient echo (MP-RAGE) sequence [time of repetition (TR) = 2400 ms, echo time (TE = 2.38 ms), inversion time (TI) = 1000 ms flip angle = 8 degrees, 162 slices, and voxel size = 1 x 1 x 1 mm^3 for volumetric analyses.

2.4 Neuroimaging analysis

The T_1-weighted MR images were processed with Freesurfer version 5.1.0 (Fischl et al., 2012) to obtain a high-resolution gray matter parcellation. The diffusion-weighted MR images were processed with a pipeline including FSL 5.0 (Jenkinson et al., 2012) and custom software, described as follows. First, FSL eddy correct was used to correct for motion and eddy currents by registering each diffusion-weighted volume to the first baseline with an affine

Topological organization of whole-brain white matter in HIV infection (doi: 10.1089/brain.2016.0457)
This paper has been peer-reviewed and accepted for publication, but has yet to undergo copyediting and proof correction. The final published version may differ from this proof.

transformation. The gradient-encoding vectors were also rotated to account for the spatial transformation of each volume (Leemans et al., 2009). Then, FSL BET was run for brain extraction, and XFIBRES was run to obtain ball-and-sticks diffusion models in each voxel (Behrens et al., 2007). Model fitting was performed with two stick compartments to improve tractography in areas with complex anatomy, such as crossing fibers. Whole-brain deterministic streamline tractography was performed to obtain geometric models of white matter pathways.

Tractography was executed utilizing an extension of the standard streamline approach to use multiple fibers per voxel with the following parameters: four seeds per voxel, an angle threshold of 50 degrees, a minimum length of 10 mm, and a minimum volume fraction of 0.1. During tracking, a kernel regression estimation framework (Cabeen et al., 2016) was used for smooth interpolation of the multi-fiber ball-and-sticks models with a Gaussian kernel using a spatial bandwidth of 1.5 mm and voxel neighborhood of 7x7x7. Then a subject-specific structural network model was constructed from the combination of diffusion MR tractography and T_1-weighted MRI gray matter labels from the Desikan-Killiany atlas (Desikan et al., 2006) and subcortical segmentations obtained from Freesurfer. For each pair of regions, a structural connection was defined by first selecting fibers with endpoints in pairs of gray matter areas and then computing the average FBL of the selected fibers to represent connection strength (Correia et al. 2008). To avoid resampling artifacts, the tractography was performed in native space and then the curve data were transformed to T_1-space to test for intersection with gray matter regions. This step registered the T_1-weighted MRI to the average baseline diffusion scan using FSL FLIRT with the mutual information criteria and an affine transformation. The resulting weighted undirected connectivity matrix was analyzed with the Brain Connectivity Toolbox (http://https://sites.google.com/site/bctnet/) to obtain global network measures of connection

strength, structural segregation (clustering coefficient), and structural integration (characteristic path length and global efficiency) (Figure 1; Rubinov & Sporns 2010).

2.5 Neuropsychological evaluation

The neuropsychological battery included tests of the following domains: Learning/recall- (1) Hopkins Verbal Learning Test-Revised (HVLT-R; Brandt & Benedict 2001), and (2) Brief Visuospatial Memory Test-Revised (BVMT-R; Benedict et al., 1996). Total correct on the immediate and delayed recall trials were defined as the dependent variables for the HVLT-R and BVMT-R. Psychomotor/processing speed- (1) Color Trails 1 (D'Elia et al., 1996), (2) Trail Making Test A (Reitan, 1955), and (3) Digit Symbol (Wechsler, 2008). Time to completion was the dependent variable for Color Trails 1 and Trail Making Test A. Total correct was the dependent variable for Digit Symbol. Executive function- (1) Color Trails 2 (D'Elia et al., 1996), and (2) Wisconsin Card Sorting Test (WCST; Grant & Berg, 1993). Time to completion was the dependent variable for Color Trails 2, and total perseveration errors served as the dependent variable for the WCST. Visuospatial skills- Block Design from the WAIS-IV (Wechsler 1997). Total correct was the dependent variable. Fine motor skills and dexterity- Grooved Pegboard Test (GPT; Kløve, 1963) non-dominant hand. Time to completion was the dependent variable.

2.6 Determination of domain specific and global neuropsychological function

For data reduction purposes, raw data from the neuropsychological test battery were converted to T scores using mean and standard deviations from a sample of 52 HIV– individuals recruited from South Africa. A deficit score (ranging from 0-5 with a score of 0 indicating normal range and greater scores indicating greater impairment) for each test was determined using the methods previously reported by Carey and colleagues (2004). This approach provides a more sensitive method for generating a summary neuropsychological score than averaging

neuropsychological scores (Carey et al., 2004; Heaton et al. 2004). A GDS was then obtained for each participant, with higher scores indicative of greater impairment. A GDS provides a continuous measure of impairment with scores > 0.5 providing high rates of specificity (0.89) and positive predictive value (0.83) in establishing HIV-associated impairment (Carey et al., 2004; Heaton et al., 2004).

Domain specific deficit scores were calculated using similar methods as the calculation for the GDS. Specifically, standardized T scores for each neuropsychological test were converted to a deficit score between 0-5. The deficit scores were averaged to determine domain specific deficit scores (i.e., learning/recall, psychomotor/processing speed, executive function, fine motor skills and dexterity, and visuospatial skills).

2.7 Statistical Analysis

All statistical analyses were conducted utilizing SPSS, version 24. Differences in age, sex, and education between HIV+ and HIV– participants were examined using independent sample t-tests (age and education) and chi-squared analyses (sex) to determine potential covariates for the primary analyses. Differences in whole-brain topological organization between groups were examined using three separate analyses of covariance or multivariate analyses of covariance (ANCOVA/MANCOVA) models, depending on the number of metrics in each category. HIV serostatus served as the independent variable and individual measures of topological organization served as dependent variables in each analysis, with intracranial volume (ICV) as a covariate. The measures of topological organization included structural segregation (clustering coefficient), structural integration (characteristic path length and global efficiency), and connection strength. Viral load was natural log transformed to achieve a normal distribution for correlation analyses. Pearson's correlations were used to determine if individual measures of

connectivity were significantly related to HIV clinical variables (CD4 T-cell count and log transformed viral load).

With respect to the distribution of GDS and domain specific deficit scores, the standardized skewness coefficients and the standardized kurtosis coefficients revealed significant departures from normality in the entire sample and within the HIV+ group. Therefore, a nonparametric procedure, the Spearman's rank order correlation (i.e., Spearman's rho), was performed to address all correlations that included the GDS or domain scores. These analyses were performed within the HIV+ sample as well as collapsed across the HIV+ and HIV– groups.

3.0 Results

Subject characteristics are listed in Table 1. There were no statistically significant differences in demographic factors (age, education, and sex) between HIV+ and HIV– participants. The ANCOVA/MANCOVA models revealed significantly weaker structural segregation in HIV+ participants, defined by a lower clustering coefficient ($F(1,42) = 11.20$, $p = 0.002$), *Cohen's d* = 1.06), as well as weaker structural integration defined by higher characteristic path length and lower global efficiency (Wilks' $\Lambda = 0.77$, $F(2,41)= 6.10$, $p = 0.005$, $d = 0.79$), with characteristic path length $F(1,42)= 12.23$, $p = 0.001$, $d = 1.12$) and global efficiency $F(1,41)= 12.33$, $p = 0.001$, $d = 1.12$) both significantly contributing to the model. Lastly, HIV+ participants showed weaker connection strength ($F(1,42) = 8.29$, $p = 0.006$, $d = 0.92$) (Table 2). Pearson's correlational analyses revealed that CD4 T-cell count and viral load were not significantly associated with any individual measures of connectivity (*r values* < |0.30|; *p values* > 0.05).

Relationships Between GDS Scores and Connectivity Metrics

Collapsed across HIV+ and HIV– participants, Spearman's rho revealed statistically

significant correlations between GDS scores with global characteristic path length ($r = 0.34$, $p = 0.027$) and mean connection strength ($r = –0.31$, $p = 0.046$). Trend level relationships were also observed with global efficiency ($r = –0.30$, $p = 0.057$) and clustering coefficient ($r = –0.30$, $p = 0.055$). Together, these results indicate that poorer cognitive performance is associated with abnormal network indices. When examined specifically within the HIV+ sample, Spearman's rho showed statistically significant negative relationships between the GDS and the clustering coefficient ($r = –0.40$, $p = 0.042$), and trend level negative associations with global efficiency ($r = –0.38$, $p = 0.056$) and connection strength ($r = –0.37$, $p = 0.062$). A trend level positive relationship was observed between the GDS and characteristic path length ($r = 0.37$, $p = 0.060$).

Relationships Between Domain-specific Deficit Scores and Connectivity Metrics

Collapsed across HIV+ and HIV– participants, poorer learning/recall was significantly associated with higher global characteristic path length ($r = 0.36$, $p = 0.010$), lower mean connection strength ($r = –0.37$, $p = 0.012$), lower global efficiency ($r = –0.36$, $p = 0.016$) and lower clustering coefficient ($r = –0.39$, $p = 0.009$). No other significant relationships were observed between the brain connectivity metrics and psychomotor/processing speed, executive function, fine motor skills and dexterity, or visuospatial skills (*r values* < |0.30|, *p values* > 0.05). When examined specifically within the HIV+ sample, learning/recall deficit scores were significantly negatively associated with the clustering coefficient ($r = –0.40$, $p = 0.037$). Negative trend level relationships were observed between learning/recall deficit scores and mean connection strength ($r = –0.36$, $p = 0.064$) and global efficiency ($r = –0.36$, $p = 0.058$), whereas a trend level positive relationship was observed with global characteristic length ($r = 0.36$, $p = 0.052$). No significant relationships were observed between the connectivity metrics and psychomotor/processing speed, executive function, fine motor skills and dexterity, or

visuospatial skills (*r values* < |0.30|, *p values* > 0.05) in the HIV+ sample.

4.0 Discussion

The current study revealed topological disorganization of brain white matter in HIV, including abnormalities in structural segregation, structural integration, and connection strength. Further, these abnormalities in network connectivity metrics were significantly associated with cognitive dysfunction both across the entire sample and specifically within the HIV+ group. These abnormalities were not significantly related to HIV clinical status (CD4 T-cell count and viral load). Findings indicate that younger HIV+ participants with limited or no antiretroviral treatment history exhibit significantly altered measures of whole-brain connectivity relative to demographically similar HIV– controls. These data suggest that alterations in whole-brain network disruption are behaviorally relevant in the context of HIV.

Structural segregation refers to neural processing within interconnected regions of the brain, whereas structural integration refers to the potential to rapidly combine specialized information from distributed brain networks. The interplay of segregation and integration in brain networks generates information that is simultaneously diversified and synthesized, resulting in patterns of high complexity. Extensive research indicates that the dynamic patterns generated by these networks provide the basis for cognition and perception (Bressler & Kelso, 2001; Frackowiak, 2004; McIntosh, 1999; Varela, Lachaux, Rodriguez, & Martinerie, 2001). Underlying these global properties is a measure of connectivity between brain regions, which we examined with the average FBL of tractography curves. Overall lower structural segregation (clustering coefficient), structural organization (characteristic path length and global efficiency), and connection strength were observed, indicating that HIV is associated with abnormal whole-brain network connectivity.

Neuroimaging studies have revealed consistent disruptions to subcortical and cortical brain structures among individuals infected with HIV (Archibald et al., 2004; Stout et al., 1998; Berger and Arendt 2000; Ances, Ortega, Vaida, Heaps, & Paul, 2012; Becker et al., 2011; Cohen et al., 2010; Ragin et al., 2012; Heaps et al., 2012). Specifically, reduced volumes have been observed within the thalamus, caudate, putamen, hippocampus, cortical white matter, and gray matter (Ances, Ortega, Vaida, Heaps, & Paul, 2012; Holt et al., 2012; Ortega et al., 2013; Paul et al., 2008; Paul et al., 2016; Thompson et al., 2005). Individuals with more advanced disease exhibit reduced cortical thickness in primary sensory and motor areas (Thompson et al., 2005), possibly reflecting distal effects of basal ganglia damage. Results from Jahanshad et al. (2012) revealed pronounced white matter network disruption in primary motor and sensory areas of the parietal and frontal lobes of older HIV individuals on stable treatment. Our study extends previous work by revealing global network disruption in younger HIV+ individuals with immune suppression and limited or no treatment history.

DTI abnormalities observed using scalar metrics in frontal, callosal, and deep white matter regions in HIV+ individuals have been associated with poor cognitive performance (Chang et al., 2008; Chen et al., 2009; Müller-Oehring et al., 2010; Pomara et al., 2001; Thurnher et al., 2005; reviewed in Hardy and Hinkin, 2002; Hoare et al., 2015; Jernigan et al., 1993; Ortega et al., 2013; Stout et al., 1998). Our results reveal a strong association between cognitive dysfunction and diffuse brain network disruption in HIV+ young adults. Collapsed across HIV+ and HIV– participants, we observed significant associations between both GDS and learning/recall with structural integration (characteristic path length) and connection strength, indicative of reduced information transfer across networks (Latora and Marchiori, 2001) and reduced FBL. Conversely, the most prominent relationships in the HIV+ group were observed between

structural segregation (clustering coefficient) and both global neuropsychological impairment as well as learning/recall. This pattern of structural abnormalities provides evidence of cognitive impairment related to a measure of neural processing within densely interconnected networks.

Inflammation is hypothesized to be one of many important drivers of neuronal injury and loss in HIV. Inflammation occurs soon after viral entry into the central nervous system (CNS) and is associated with the release of proinflammatory cytokines, chemokines, and neurotoxic viral proteins in response to HIV-infected macrophages and microglia (Anthony et al., 2005; Lentz et al., 2011; Sailasuta et al., 2012; Harezlak et al., 2011; Valcour et al., 2012; Vera et al., 2016). In turn, these activate uninfected macrophages and microglia to further release neurotoxic substances that lead to compromised synaptodendritic connections, damage to axonal and myelin integrity, and potentially neuronal death (Conant et al., 1998; Raja et al., 1997). These injuries are distributed widely throughout the brain and correspond to white matter damage (Ellis, Langford, & Masliah, 2007) as well as cognitive impairment (Everall et al., 1999).

An advantage of our study is the tractography method employed to quantify structural connectivity. Typically, a major challenge of estimating whole-brain connectivity metrics is the presence of complex configurations of fiber bundle anatomy such as fiber crossings. The diffusion tensor model does not accurately represent voxels consisting of multiple fiber populations, which limits the anatomical validity of network models derived using single tensor models. More sophisticated techniques that represent multiple fibers, such as multi-compartment and high angular resolution diffusion imaging, offer greater anatomical accuracy and improved sensitivity in detecting complex anatomical features related to white matter changes due to disease (Tuch et al., 1999; Tuch et al., 2002). We used the ball-and-sticks multi-compartment model (Behrens et al., 2007) and a model-based estimation framework (Cabeen et al., 2016) to

Topological organization of whole-brain white matter in HIV infection (doi: 10.1089/brain.2016.0457)
This paper has been peer-reviewed and accepted for publication, but has yet to undergo copyediting and proof correction. The final published version may differ from this proof.

improve the accuracy of connectivity mapping. Importantly, while this approach is ideal for the single shell data, more sophisticated microstructure models that utilize multi-shell acquisitions may provide improved anatomical accuracy and sensitivity to detect white matter changes. Future studies may benefit by using neurite orientation dispersion and density imaging (NODDI) to characterize changes in neurite density and orientation dispersion (Zhang et al., 2012).

Several limitations are important to address. First, we did not have sufficient numbers of male HIV+ participants to examine sex differences in brain network topology. Previous research conducted in HIV– populations reveals sex differences in brain topology (Gong et al., 2009; Yan et al., 2010), emphasizing the importance of examining sex differences in future studies. Additionally, future research is needed to determine whether treatment improves whole-brain connectivity abnormalities. Lastly, we excluded participants with substance use disorder due to evidence that structural connectivity is disrupted in substance users independent of HIV (Bava et al., 2009; Kim et al., 2014). Our approach ensured that the observed effects were not confounded by substance use. However, our results may not generalize to the population of HIV+ substance users. Despite these limitations, our findings provide strong evidence for functionally relevant disruptions to network organization in HIV.

5.0 Conclusions

The current manuscript extends the literature in three novel ways. First, our cohort was comprised of young HIV+ adults. Second, our sample was predominantly free of treatment confounds on brain connectivity. Lastly, the present study included measures of cognition that inform the functional relevance of the connectivity measures. Collectively, the results support a model of diffuse network changes in young HIV+ individuals with limited or no treatment history and corresponding cognitive dysfunction. The results provide further evidence of the

utility of anatomical brain connectivity as a noninvasive biomarker of white matter disruption in HIV infection.

Acknowledgments

There are no actual or potential conflicts of interest for any of the authors on this manuscript. Funding was supported by the National Institute of Mental Health (MH085604). Dr. Stein is supported by the Medical Research Council of South Africa.

This article has been peer-reviewed and accepted for publication, but has yet to undergo copyediting and proof correction. The final published version may differ from this proof.
Topological organization of whole-brain white matter in HIV infection (doi: 10.1089/brain.2016.0457)

References

Ances, B. M., Ortega, M., Vaida, F., Heaps, J., & Paul, R. (2012). Independent effects of HIV, aging, and HAART on brain volumetric measures. *Journal of acquired immune deficiency syndromes (1999)*, *59*(5), 469.

Anthony, I. C., Ramage, S. N., Carnie, F. W., Simmonds, P., & Bell, J. E. (2005). Influence of HAART on HIV-related CNS disease and neuroinflammation. *Journal of Neuropathology & Experimental Neurology*, *64*(6), 529-536.

Archibald, S. L., Masliah, E., Fennema-Notestine, C., Marcotte, T. D., Ellis, R. J., McCutchan, J. A., ... & Jernigan, T. L. (2004). Correlation of in vivo neuroimaging abnormalities with postmortem human immunodeficiency virus encephalitis and dendritic loss. *Archives of Neurology*, *61*(3), 369-376.

Avdoshina, V., Bachis, A., & Mocchetti, I. (2013). Synaptic dysfunction in human immunodeficiency virus type- 1- positive subjects: inflammation or impaired neuronal plasticity? *Journal of internal medicine*, *273*(5), 454-465.

Bassett, D. S., Bullmore, E., Verchinski, B. A., Mattay, V. S., Weinberger, D. R., & Meyer-Lindenberg, A. (2008). Hierarchical organization of human cortical networks in health and schizophrenia. *The Journal of Neuroscience*, *28*(37), 9239-9248.

Bassett, D. S. (2010). Clinical applications of complex network analysis. *Short Course III-Analysis and Function of Large-Scale Brain Networks, Washington, DC, USA: Society for Neuroscience*, 55-63.

Bava, S., Frank, L. R., McQueeny, T., Schweinsburg, B. C., Schweinsburg, A. D., & Tapert, S. F. (2009). Altered white matter microstructure in adolescent substance users. Psychiatry Research: Neuroimaging, 173(3), 228-237.

Becker, J. T., Sanders, J., Madsen, S. K., Ragin, A., Kingsley, L., Maruca, V., ... & Sacktor, N. (2011). Subcortical brain atrophy persists even in HAART-regulated HIV disease. *Brain imaging and behavior*, *5*(2), 77-85.

Behrens, T. E. J., Berg, H. J., Jbabdi, S., Rushworth, M. F. S., & Woolrich, M. W. (2007). Probabilistic diffusion tractography with multiple fibre orientations: What can we gain?. Neuroimage, 34(1), 144-155.

Brandt, J., & Benedict, R. H. (2001). *Hopkins verbal learning test--revised: professional manual*. Psychological Assessment Resources.

Benedict, R. H., Schretlen, D., Groninger, L., Dobraski, M., & Shpritz, B. (1996). Revision of the Brief Visuospatial Memory Test: Studies of normal performance, reliability, and validity. *Psychological Assessment*, *8*(2), 145.

Berger, J. R., & Arendt, G. (2000). HIV dementia: the role of the basal ganglia and dopaminergic systems. *Journal of Psychopharmacology*, *14*(3), 214-221.

Bressler, S. L., & Kelso, J. S. (2001). Cortical coordination dynamics and cognition. *Trends in cognitive sciences*, *5*(1), 26-36.

Bullmore, E., & Sporns, O. (2009). Complex brain networks: graph theoretical analysis of structural and functional systems. *Nature Reviews Neuroscience*, *10*(3), 186-198.

Cabeen, R. P., Bastin, M. E., & Laidlaw, D. H. (2016). Kernel regression estimation of fiber orientation mixtures in diffusion MRI. *NeuroImage*, *127*, 158-172.

Carey, C. L., Woods, S. P., Gonzalez, R., Conover, E., Marcotte, T. D., Grant, I., & Heaton, R. K. (2004). Predictive validity of global deficit scores in detecting neuropsychological impairment in HIV infection. *Journal of clinical and experimental neuropsychology*, *26*(3), 307-319.

Chang, L., Wong, V., Nakama, H., Watters, M., Ramones, D., Miller, E. N., ... & Ernst, T. (2008). Greater than age-related changes in brain diffusion of HIV patients after 1 year. *Journal of Neuroimmune Pharmacology*, *3*(4), 265-274.

Chen, Y., An, H., Zhu, H., Stone, T., Smith, J. K., Hall, C., ... & Lin, W. (2009). White matter abnormalities revealed by diffusion tensor imaging in non-demented and demented HIV+ patients. *Neuroimage*, *47*(4), 1154-1162.

Cohen, R. A., Harezlak, J., Schifitto, G., Hana, G., Clark, U., Gongvatana, A., ... & Brown, M. (2010). Effects of nadir CD4 count and duration of human immunodeficiency virus infection on brain volumes in the highly active antiretroviral therapy era. *Journal of neurovirology*, *16*(1), 25-32.

Conant K, Garzino-Demo A, Nath A, et al. Induction of monocyte chemoattractant protein-1 in HIV-1 Tat-stimulated astrocytes and elevation in AIDS dementia. Proc Natl Acad Sci U S A 1998;95:3117–3121.

Correia, S., Lee, S. Y., Voorn, T., Tate, D. F., Paul, R. H., Zhang, S., ... & Laidlaw, D. H. (2008). Quantitative tractography metrics of white matter integrity in diffusion-tensor MRI. Neuroimage, 42(2), 568-581.

D'Elia, L., & Satz, P. (1996). *Color trails test*. Psychological Assessment Resources.

Desikan, R. S., Ségonne, F., Fischl, B., Quinn, B. T., Dickerson, B. C., Blacker, D., ... & Killiany, R. J. (2006). An automated labeling system for subdividing the human cerebral cortex on MRI scans into gyral based regions of interest. Neuroimage, 31(3), 968-980.

Ellis, R., Langford, D., & Masliah, E. (2007). HIV and antiretroviral therapy in the brain: neuronal injury and repair. *Nature Reviews Neuroscience*, *8*(1), 33-44.

Everall, I.P., Heaton, R.K., Marcotte, T.D., Ellis, R.J., McCutchan, J.A., Atkinson, J.H., … & HRNC Group (1999). Cortical synaptic density is reduced in mild to moderate human immunodeficiency virus neurocognitive disorder. *Brain Pathology*, *9*(2), 209-217.

Everall, I., Vaida, F., Khanlou, N., Lazzaretto, D., Achim, C., Letendre, S., ... & Morgello, S. (2010). Cliniconeuropathologic correlates of human immunodeficiency virus in the era of antiretroviral therapy. *Journal of neurovirology*.

Filippi, C. G., Uluğ , A. M., Ryan, E., Ferrando, S. J., & van Gorp, W. (2001). Diffusion tensor imaging of patients with HIV and normal-appearing white matter on MR images of the brain. *American Journal of Neuroradiology*, *22*(2), 277-283.

Fischl, B. (2012). FreeSurfer. Neuroimage, 62(2), 774-781.

Ford, N., Calmy, A., & Mills, E. J. (2011). The first decade of antiretroviral therapy in Africa. Globalization and health, 7(1), 1.

Frackowiak, R. S. (2004). *Human brain function*. K. J. Friston, C. D. Frith, R. J. Dolan, C. J. Price, S. Zeki, J. T. Ashburner, & W. D. Penny (Eds.). Academic press.

Gong, G., He, Y., Concha, L., Lebel, C., Gross, D. W., Evans, A. C., & Beaulieu, C. (2009). Mapping anatomical connectivity patterns of human cerebral cortex using in vivo diffusion tensor imaging tractography. *Cerebral cortex*, *19*(3), 524-536.

Gongvatana, A., Schweinsburg, B. C., Taylor, M. J., Theilmann, R. J., Letendre, S. L., Alhassoon, O. M., ... & Frank, L. R. (2009). White matter tract injury and cognitive impairment in human immunodeficiency virus–infected individuals. *Journal of neurovirology*.

Grant, D. A., & Berg, E. A. (1993). *Wisconsin Card Sorting Test (WCST)*. PAR.

Hardy, D. J., & Hinkin, C. H. (2002). Reaction time performance in adults with HIV/AIDS. *Journal of Clinical and Experimental Neuropsychology*, *24*(7), 912-929.

Harezlak, J., Buchthal, S., Taylor, M., Schifitto, G., Zhong, J., Daar, E. S., ... & Cohen, R. (2011). Persistence of HIV− Associated Cognitive Impairment, Inflammation and Neuronal Injury in era of Highly Active Antiretroviral Treatment. *AIDS (London, England)*, *25*(5), 625.

He, Y., Chen, Z., & Evans, A. (2008). Structural insights into aberrant topological patterns of large-scale cortical networks in Alzheimer's disease. *The Journal of neuroscience*, *28*(18), 4756-4766.

Heaps, J. M., Joska, J., Hoare, J., Ortega, M., Agrawal, A., Seedat, S., ... & Paul, R. (2012). Neuroimaging markers of human immunodeficiency virus infection in South Africa. *Journal of neurovirology*, *18*(3), 151-156.

Heaton, R. K., Marcotte, T. D., Mindt, M. R., Sadek, J., Moore, D. J., Bentley, H., ... & Grant, I. (2004). The impact of HIV-associated neuropsychological impairment on everyday functioning. *Journal of the International Neuropsychological Society*, *10*(03), 317-331.

Heaton, R. K., Franklin, D. R., Ellis, R. J., McCutchan, J. A., Letendre, S. L., LeBlanc, S., ... & Collier, A. C. (2011). HIV-associated neurocognitive disorders before and during the era of combination antiretroviral therapy: differences in rates, nature, and predictors. *Journal of neurovirology*, *17*(1), 3-16.

Harezlak, J., Buchthal, S., Taylor, M., Schifitto, G., Zhong, J., Daar, E. S., ... & Cohen, R. (2011). Persistence of HIV− Associated Cognitive Impairment, Inflammation and Neuronal Injury in era of Highly Active Antiretroviral Treatment. *AIDS (London, England)*, *25*(5), 625.

Hoare, J., Fouche, J. P., Spottiswoode, B., Sorsdahl, K., Combrinck, M., Stein, D. J., ... & Joska, J. A. (2011). White-matter damage in clade C HIV-positive subjects: a diffusion tensor imaging study. *The Journal of neuropsychiatry and clinical neurosciences*.

Hoare, J., Fouche, J. P., Phillips, N., Joska, J. A., Paul, R., Donald, K. A., ... & Stein, D. J. (2015). White matter micro-structural changes in ART-naive and ART-treated children and adolescents infected with HIV in South Africa. *AIDS*, *29*(14), 1793-1801.

Holt, J. L., Kraft-Terry, S. D., & Chang, L. (2012). Neuroimaging studies of the aging HIV-1-infected brain. *Journal of neurovirology*, *18*(4), 291-302.

Jahanshad, N., Valcour, V. G., Nir, T. M., Kohannim, O., Busovaca, E., Nicolas, K., & Thompson, P. M. (2012). Disrupted brain networks in the aging HIV+ population. *Brain connectivity*, *2*(6), 335-344.

Jenkinson, M., Beckmann, C. F., Behrens, T. E., Woolrich, M. W., & Smith, S. M. (2012). Fsl. Neuroimage, 62(2), 782-790.

Jernigan, T. L., Archibald, S., Hesselink, J. R., Atkinson, J. H., Velin, R. A., McCutchan, J. A., ... & Grant, I. (1993). Magnetic resonance imaging morphometric analysis of cerebral volume loss in human immunodeficiency virus infection. *Archives of neurology*, *50*(3), 250-255.

Kaul, M., & Lipton, S. A. (2006). Mechanisms of neuroimmunity and neurodegeneration associated with HIV-1 infection and AIDS. *Journal of Neuroimmune Pharmacology*, *1*(2), 138-151.

Kim, J., Parker, D., Whyte, J., Hart, T., Pluta, J., Ingalhalikar, M., ... & Verma, R. (2014). Disrupted structural connectome is associated with both psychometric and real-world neuropsychological

impairment in diffuse traumatic brain injury. *Journal of the International Neuropsychological Society*, *20*(09), 887-896.

Kløve, H. (1963). Grooved pegboard. *Lafayette, IN: Lafayette Instruments*.

Latora, V., & Marchiori, M. (2001). Efficient behavior of small-world networks. Physical review letters, 87(19), 198701.

Leemans, A., & Jones, D. K. (2009). The B- matrix must be rotated when correcting for subject motion in DTI data. Magnetic Resonance in Medicine, 61(6), 1336-1349.

Lentz, M. R., Kim, W. K., Kim, H., Soulas, C., Lee, V., Venna, N., ... & Gonzalez, R. G. (2011). Alterations in brain metabolism during the first year of HIV infection. Journal of neurovirology, 17(3), 220-229.

Lo, C. Y., Wang, P. N., Chou, K. H., Wang, J., He, Y., & Lin, C. P. (2010). Diffusion tensor tractography reveals abnormal topological organization in structural cortical networks in Alzheimer's disease. *The Journal of Neuroscience*, *30*(50), 16876-16885.

Masliah, E., Ellis, R. J., Mallory, M., Heaton, R. K., Marcotte, T. D., Nelson, J. A., ... & McCutchan, J. A. (1997). Dendritic injury is a pathological substrate for human immunodeficiency virus—related cognitive disorders. *Annals of neurology*, *42*(6), 963-972.

McIntosh, A. R. (1999). Mapping cognition to the brain through neural interactions. *Memory*, *7*(5-6), 523-548.

Müller-Oehring, E. M., Schulte, T., Rosenbloom, M. J., Pfefferbaum, A., & Sullivan, E. V. (2010). Callosal degradation in HIV-1 infection predicts hierarchical perception: a DTI study. *Neuropsychologia*, *48*(4), 1133-1143.

Ortega, M., Heaps, J. M., Joska, J., Vaida, F., Seedat, S., Stein, D. J., ... & Ances, B. M. (2013). HIV clades B and C are associated with reduced brain volumetrics. *Journal of neurovirology*, *19*(5), 479-487.

Paul, R. H., Ernst, T., Brickman, A. M., Yiannoutsos, C. T., Tate, D. F., Cohen, R. A., & Navia, B. A. (2008). Relative sensitivity of magnetic resonance spectroscopy and quantitative magnetic resonance imaging to cognitive function among nondemented individuals infected with HIV. *Journal of the International Neuropsychological Society*, *14*(05), 725-733.

Paul, R. H., Phillips, S., Hoare, J., Laidlaw, D. H., Cabeen, R., Olbricht, G. R., ... & Salminen, L. E. (2016). Neuroimaging abnormalities in clade C HIV are independent of Tat genetic diversity. *Journal of NeuroVirology*, 1-10.

Pomara, N., Crandall, D.T., Choi, S.J., Johnson, G., & Lim, K.O. (2001). White matter abnormalities in HIV-1 infection: a diffusion tensor imaging study. *Psychiatry Research: Neuroimaging*, 106(1), 15-24.

Ragin, A. B., Storey, P., Cohen, B. A., Epstein, L. G., & Edelman, R. R. (2004). Whole brain diffusion tensor imaging in HIV-associated cognitive impairment. *American Journal of Neuroradiology*, *25*(2), 195-200.

Ragin, A. B., Du, H., Ochs, R., Wu, Y., Sammet, C. L., Shoukry, A., & Epstein, L. G. (2012). Structural brain alterations can be detected early in HIV infection. *Neurology*, *79*(24), 2328-2334.

Raja F, Sherriff FE, Morris CS, et al. Cerebral white matter damage in HIV infection demonstrated using beta-amyloid precursor protein immunore-activity. Acta Neuropathol (Berl). 1997;93:184–189.

Reda, A. A., & Biadgilign, S. (2012). Determinants of adherence to antiretroviral therapy among HIV-infected patients in Africa. AIDS Research and treatment, 2012.

Reitan, R. M. (1955). The relationship of the Trail Making Test to organic brain damage. *Journal of Consulting Psychology*, *19*, 393-394.

Rubinov, M., & Sporns, O. (2010). Complex network measures of brain connectivity: uses and interpretations. Neuroimage, 52(3), 1059-1069.

Stout, J. C., Ellis, R. J., Jernigan, T. L., Archibald, S. L., Abramson, I., Wolfson, T., ... & Grant, I. (1998). Progressive cerebral volume loss in human immunodeficiency virus infection: a longitudinal volumetric magnetic resonance imaging study. *Archives of neurology*, *55*(2), 161-168.

Sailasuta, N., Ross, W., Ananworanich, J., Chalermchai, T., DeGruttola, V., Lerdlum, S., ... & Spudich, S. (2012). Change in brain magnetic resonance spectroscopy after treatment during acute HIV infection. PloS one, 7(11), e49272.

Sheehan, D. V., Lecrubier, Y., Sheehan, K. H., Amorim, P., Janavs, J., Weiller, E., ... & Dunbar, G. C. (1998). The Mini-International Neuropsychiatric Interview (MINI): the development and validation of a structured diagnostic psychiatric interview for DSM-IV and ICD-10. *Journal of clinical psychiatry*.

Stebbins, G. T., Smith, C. A., Bartt, R. E., Kessler, H. A., Adeyemi, O. M., Martin, E., ... & Moseley, M. E. (2007). HIV-associated alterations in normal-appearing white matter: a voxel-wise diffusion tensor imaging study. *JAIDS Journal of Acquired Immune Deficiency Syndromes*, *46*(5), 564-573.

Thompson, P. M., Dutton, R. A., Hayashi, K. M., Toga, A. W., Lopez, O. L., Aizenstein, H. J., & Becker, J. T. (2005). Thinning of the cerebral cortex visualized in HIV/AIDS reflects CD4+ T lymphocyte decline. *Proceedings of the National Academy of Sciences*, *102*(43), 15647-15652.

Thurnher, M. M., Castillo, M., Stadler, A., Rieger, A., Schmid, B., & Sundgren, P. C. (2005). Diffusion-tensor MR imaging of the brain in human immunodeficiency virus–positive patients. *American journal of neuroradiology*, *26*(9), 2275-2281.

Tuch, D. S., Weisskoff, R. M., Belliveau, J. W., & Wedeen, V. J. (1999, May). High angular resolution diffusion imaging of the human brain. In *Proceedings of the 7th Annual Meeting of ISMRM, Philadelphia* (Vol. 321).

Tuch, D. S., Reese, T. G., Wiegell, M. R., Makris, N., Belliveau, J. W., & Wedeen, V. J. (2002). High angular resolution diffusion imaging reveals intravoxel white matter fiber heterogeneity. *Magnetic Resonance in Medicine*, *48*(4), 577-582.

Varela, F., Lachaux, J. P., Rodriguez, E., & Martinerie, J. (2001). The brainweb: phase synchronization and large-scale integration. *Nature reviews neuroscience*, *2*(4), 229-239.

Valcour, V., Chalermchai, T., Sailasuta, N., Marovich, M., Lerdlum, S., Suttichom, D., ... & van Griensven, F. (2012). Central nervous system viral invasion and inflammation during acute HIV infection. *Journal of Infectious Diseases*, *206*(2), 275-282.

Vera, J. H., Guo, Q., Cole, J. H., Boasso, A., Greathead, L., Kelleher, P., ... & Matthews, P. M. (2016). Neuroinflammation in treated HIV-positive individuals A TSPO PET study. *Neurology*, *86*(15), 1425-1432.

Wechsler III, D. WAIS-III Administration and Scoring Manual. San Antonio, TX: The Psychological Corporation, 1997.

Wechsler, D., Coalson, D. L., & Raiford, S. E. (2008). *WAIS-IV: Wechsler adult intelligence scale*. San Antonio, TX: Pearson.

Wright, P., Heaps, J., Shimony, J. S., Thomas, J. B., & Ances, B. M. (2012). The effects of HIV and combination antiretroviral therapy on white matter integrity. *AIDS (London, England)*, *26*(12), 1501.

Yan, C., Gong, G., Wang, J., Wang, D., Liu, D., Zhu, C., ... & He, Y. (2011). Sex-and brain size–related small-world structural cortical networks in young adults: a DTI tractography study. *Cerebral cortex*, *21*(2), 449-458.

Yu, Q., Sui, J., Rachakonda, S., He, H., Pearlson, G., & Calhoun, V. D. (2011). Altered small-world brain networks in temporal lobe in patients with schizophrenia performing an auditory oddball task. *Frontiers in systems neuroscience*, *5*, 7.

Zhang, J., Wang, J., Wu, Q., Kuang, W., Huang, X., He, Y., & Gong, Q. (2011). Disrupted brain connectivity networks in drug-naive, first-episode major depressive disorder. *Biological psychiatry*, *70*(4), 334-342

Zhang, H., Schneider, T., Wheeler-Kingshott, C. A., & Alexander, D. C. (2012). NODDI: practical in vivo neurite orientation dispersion and density imaging of the human brain. Neuroimage, 61(4), 1000-1016.

Brain Connectivity
Topological organization of whole-brain white matter in HIV infection (doi: 10.1089/brain.2016.0457)
This paper has been peer-reviewed and accepted for publication, but has yet to undergo copyediting and proof correction. The final published version may differ from this proof.

Brain Connectivity

Topological organization of whole-brain white matter in HIV infection (doi: 10.1089/brain.2016.0457)

Topological organization of whole-brain white matter in HIV infection (doi: 10.1089/brain.2016.0457)

This paper has been peer-reviewed and accepted for publication, but has yet to undergo copyediting and proof correction. The final published version may differ from this proof.

Brain Connectivity
Topological organization of whole-brain white matter in HIV infection (doi: 10.1089/brain.2016.0457)

Table 2. Differences in network connectivity between HIV+ and HIV– participants

	HIV+ (n =29)	HIV– (n=16)	*p* value
Global Clustering Coefficient (mm)	53.18 (4.47)	57.67 (3.37)	0.002
Global Characteristic Path Length (1/mm)	0.015 (0.0012)	0.013 (0.0009)	0.001
Global Efficiency (mm)	77.86 (7.17)	85.62 (6.54)	0.001
Global Connection Strength (mm)	2939.75 (385.99)	3271.76 (312.58)	0.006

Note: Mean (SD)

Table 1. Subject Characteristics

	HIV+ (n=29)	HIV– (n=16)	*p* value
Mean Age ± SD (range)	25.89 ± 2.12 (22-29)	24.69 ± 4.53 (20-32)	0.55
Mean Education ± SD (range)	10.76 ± 0.69 (10-12)	10.94 ± 1.29 (7-12)	0.31
Sex (% Male)	17%	31%	0.46
Mean recent CD4 (cells/mm^3) ± SD (range)	249.79 ±164.23 (35-799)		
Mean plasma VL (copies/ml)[a] ± SD (range)	4.21 ± 1.06 (2.26-6.25)		
Mean months of infection± SD (range)	9.33 ± 19.56 (0-97)		
% Prescribed Antiretroviral Therapy	17%		
Mean Intracranial Volume (cm^3) ± SD (range)	1,307.15 ± 246.69 (1027.86-1728.54)	1,345.50 ± 211.64 (961.03-2033.13)	0.60
Mean Global Deficit Score ± SD (range)	0.34 ± 0.32 (0-1)	0.18 ± 0.22 (0-0.82)	0.06

Note: [a]Viral load $\log_{10}$ transformed

Topological organization of whole-brain white matter in HIV infection (doi: 10.1089/brain.2016.0457)
This paper has been peer-reviewed and accepted for publication, but has yet to undergo copyediting and proof correction. The final published version may differ from this proof.

Table 1. Subject Characteristics

Note: [a]Viral load $\log_{10}$ transformed

Table 2. Differences in network connectivity between HIV+ and HIV– individuals

Note: Mean (SD)

Figure 1. Structural Network Analysis Visualizations

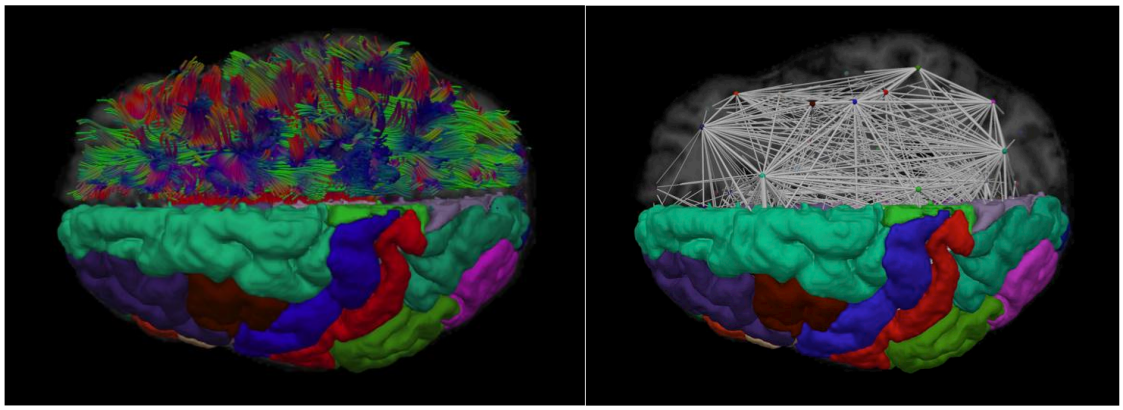

Left: A visualization of imaging-based reconstructions of anatomy, showing diffusion MRI-based tractography and T1-weighted MRI-based gray matter segmentations. The left hemisphere shows Desikan-Killiany regions-of-interest, and the right hemisphere shows streamline tractography curves used to define connectivity between regions.

Right: A visualization of a structural network model derived from neuroimaging data. The left hemisphere shows Desikan-Killiany regions-of-interest, and the right hemisphere shows a node-link diagram representing the topological organization of white matter. Nodes are placed at the centroid of each region and the links are derived from the average fiber bundle length between the pairs of regions with structural connections.

Figure 1. Structural Network Analysis Visualizations

Figure 1: Left: A visualization of imaging-based reconstructions of anatomy, showing diffusion MRI-based tractography and T1-weighted MRI-based gray matter segmentations. The left

hemisphere shows Desikan-Killiany regions-of-interest, and the right hemisphere shows streamline tractography curves used to define connectivity between regions.

Right: A visualization of a structural network model derived from neuroimaging data. The left hemisphere shows Desikan-Killiany regions-of-interest, and the right hemisphere shows a node-link diagram representing the topological organization of white matter. Nodes are placed at the centroid of each region and the links are derived from the average fiber bundle length between the pairs of regions with structural connections.

Topological organization of whole-brain white matter in HIV infection (doi: 10.1089/brain.2016.0457)
This paper has been peer-reviewed and accepted for publication, but has yet to undergo copyediting and proof correction. The final published version may differ from this proof.